Numerical Insights into Shallow Foundation Settlement on Silty Soil Stabilized with Granular Material

Rizwan Ali Soomro[1] and Sharafat Ali Darban[1]

1. School of Mechanics and Civil Engineering, China University of Mining and Technology (CUMT), Xuzhou, Jiangsu, 221116, China

DOI: https://doi.org/10.56293/IJASR.2025.6306

IJASR 2025
VOLUME 8
ISSUE 1 JANUARY - FEBRUARY **ISSN: 2581-7876**

Abstract: Silty soils are fine-grained materials that typically exhibit low strength, low hydraulic conductivity, and high compressibility, which contributes to their minimal bearing capacity. As a result, foundation failures can occur due to the insufficient strength and stiffness of silty soils. Buildings constructed on these types of soil may experience excessive settlement, which can significantly reduce their design lifespan. This excessive settlement can lead to cracks in walls and roof slabs, as well as the misalignment of doors and windows. In severe cases, it may even result in the collapse of the structure. To address these issues, this study proposes a method to enhance the bearing capacity of the existing ground by blending the silty soil with granular material at replacement rates of 20%, 30%, and 40%. Three different footing sizes were tested: (1.83 × 1.83 m²), (1.22 × 1.22 m²), and (1.22 × 1.83 m²). A three-dimensional finite element analysis was conducted to calculate the bearing capacity of the shallow foundations on the original soil, and the performance of the footings on improved ground was compared. To model soil behavior, a linear elastic perfectly plastic model utilizing the Mohr-Coulomb failure criterion was employed. The results indicated that as the size of the footing increases, the yield point also rises. The percentage improvement in ultimate bearing capacity for footings with dimensions of (1.22 × 1.22 m²), (1.83 × 1.83 m²), and (1.22 × 1.83 m²) founded on 40% blended silty clay and granular material was found to be 91%, 89%, and 83%, respectively. This study demonstrates the effectiveness of soil improvement techniques in enhancing the structural integrity of foundations situated on silty soils.

Keywords: Bearing Capacity, Foundation Failure, Soil Improvement, Finite Element Analysis

I. Introduction

Silty soils are fine-grained soils having low strength, minimal bearing capacity and low hydraulic conductivity with high compressibility. Furthermore, the swelling and shrinkage potentials make them susceptible to large settlements and deformations with time especially, when located in areas with a high-water table. When the shallow foundations (footings) of buildings are constructed on such type of silty soils which are highly compressible, it can cause excessive settlements with the passage of time resulting in the adverse effects on the super structures (buildings) performance and it can reduce the design life of the buildings. The footing is most important and the bottom most part of the foundation. The main function of the foundation is to transfer the load of the superstructure to the ground. The shear strength and stiffness of the ground are the key engineering parameters for foundation stability.

The failure of a foundation can has catastrophic consequences and special care must be taken to avoid such failure e.g. stabilise the existing weak ground blended with granular soil. For improving the weak soil properties, there are several methods. For example, the bearing capacity of soil in shallow can be increased by increasing confinement. An enclosure is formed by skirted foundations in which soil is tightly confined. Salencon [1] concluded that bearing capacity increment of a footing on cohesive soil due to rigid wall presence was little. However, substantial increment in bearing capacity of foundation on sand by increasing confinement was reported by the researchers.

Villalobos et al [2]'s experimental study shows that the settlement of a foundation can be minimised and bearing capacity can be increased with existence of skirt. Mahiyar and Patel [3] reported enhancement of baring capacity with increment of confinement depth. They observed that the onfinement became ineffective with increment of

diameter of skirt. The lateral movement is constraint due to confinement of soil under footing resulted in the stiffer behaviour of load settlement curve [4]. Sawwaf and Nazer [5] studied the behaviour of a circular footing on confined granular material. They observed that bearing capacity increased as much as 17 times higher than that of unconfined condition and significant reduction in settlement. Ortiz [6] improved the bearing capacity of the existing foundation by inserting vertical dowels around exiting foundation. A remarkable increment in bearing capacity of 20% was obtained by that method. Al-Aghabri and Zein [7] conducted tests for determining bearing capacity of strip footing resting on the ground improved with skirts. They observed improvement in the bearing capacity by three times that of original. Rajagopal et al. [8] carried out several triaxial compression tests in which sand was highly confined. They observed much improvement in strength and stiffness due to geocell confinement. Dash et al. [9] carried experiment on a strip footing resting on dense sand. It was revealed that with inclusion of geocell, the bearing capacity was improved as much as 8 times that of original. Similar experiment was repeated on circular footing [10]. In case of circular footing, the bearing capacity increased by 6 times of that original due to geocell provision. All prediction can be wrong due to swelling property of sub-grade soil in spite of correct design of the pavement. The high stresses generated due to volume changes can cause a highway to crack, heave and settlement.

Consequently, the maintenance cost can be increased so much that the road authority can be forced to reconstruct the pavement [13]. Mahipal et.al [14] studied the behavior of fiber reinforcement to improve the stability of silty sand sub-grade. Resilient modulus decreases with the application of cyclic loads and deviator stress but resilient strain increases. On the other hand, resilient modulus increases with the increase of un-coffining pressure but resilient strain decreases. Hamza Gullu [14] made a numerical study on geotextile stabilized highway embankment under vibration loading. Results showed that soft soil gave better performance by single layer of geotextile along with reasonable factor of safety. However, two or more geotextile layers can be used when highway embankment is subjected to vibration loading. Adel Djellali et.al [17] investigated the behavior of flexible pavements on expansive silty soils in Tebessa, Algeria. The numerical modelling was carried out to investigate the behaviour of pavement structure using commercial software Plaxis. In addition, calibration of model parameters was done by performing free expansion test. They concluded that performance of Mohr Coulomb and soft soil model is quite satisfactory when these are combined in predicted the pavement deformation. Soomro et al. [11] investigated the settlement behavior of shallow foundations on waterlogged soil and recommends suitable foundation types to support building loads. Three-dimensional coupled consolidation analyses revealed that footings measuring 1.22 × 1.22 m^2 and 1.83 × 1.83 m^2 had ultimate load capacities of approximately 10 kN and 21 kN, which improved significantly with pit sand, showing increases of 9 and 6 times, respectively. Among alternative foundations, the piled raft foundation achieved the highest capacity at 620 kN, providing valuable insights for safe construction practices in waterlogged conditions. Ayman A. Abed, 2008 [16] made study to model the behavior of expansive soil in the framework of unsaturated soil mechanics. The proposed model is used then to predict the displacements associated with the changes in soil suction. The elasto plasticity framework is used for constitutive modeling. Mostafa Deep Hashem 2013 [15] made study on Numerical Modeling of Flexible Pavement Constructed on Expansive Soils.

Mohr coulomb model was used to predict the displacement associated with sub grade under different drainage conditions and the results showed that the values of vertical displacement for dry drained sub grade were less than that occurs in saturated drained sub grade and dry undrained sub grade and vertical displacement was maximum under the center of different wheel load as compared to center of shoulder. Due to loading on the footing, three failure modes can be identified depending upon soil and foundation size and depth. First mode of failure is mostly found due to loading on the footings which are resting on stiff clay and dense sand. It is called general shear failure. The second is local shear failure mode which develops in medium dense and stiff clays. Thirdly punching mode of failure is generated in the loose sands and soft clays. Silty soils are fine-grained soils low strength with low hydraulic conductivity with high compressibility hence minimal bearing capacity. Foundation failure may be caused due to inadequate strength and stiffness of silty soil. Buildings constructed on silty soils may experience excessive settlement and it can reduce design life of buildings. The excessive settlement can result in cracking of the walls, roof slab and jamming of the door and windows can take place. Sometimes collapse of a building might occur. Based on the above-mentioned problems, the aim of the research to investigate settlement behavior of different size footings whose foundation is resting on silty soil. The specific objectives include comparing the bearing capacity of the footings with stabilized silty soil with granular soil with replacement 20%, 30% and 40% and finding out optimized amount of stabilizer for increased bearing capacity at allowable settlement.

2. Three-Dimensional Finite Element Analysis

To calculate and bearing capacity of the shallow foundation (footings) on exiting ground, three-dimension finite element analysis were carried out. In addition, the bearing capacity of footings on the improved ground was compared. The bearing capacities of three sizes of footings (1.83 m × 1.83 m, 1.22 m × 1.22 m and 1.22 m × 1.83 m) on existing and improved ground were computed and compared. Figures 1(a) and (b) show the elevation view of the configuration of numerical load test for a footing of typical size on the existing ground. The depth of the all the footing were taken as 1.5 m (≈ 5.0 ft).

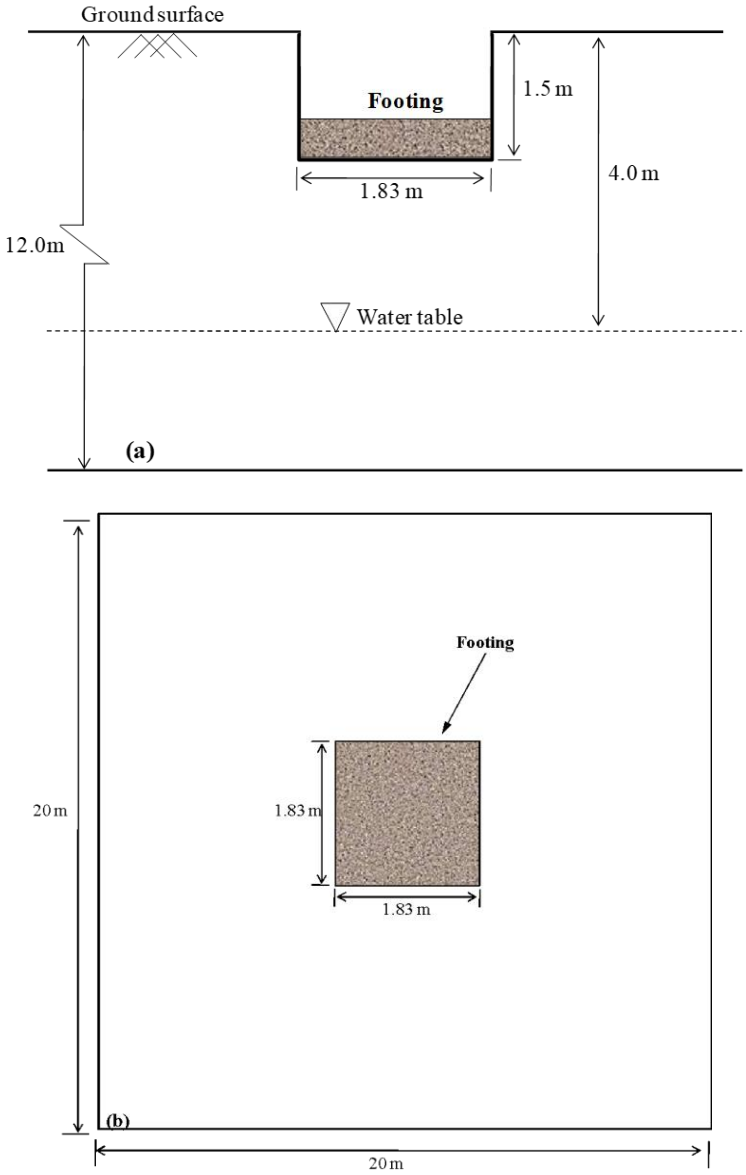

Figure 1. Geometry of the problem in the analysis (a) elevation view (b) plan view

2.1. Finite element mesh and boundary conditions

The half of finite element mesh adopted for a typical case of footing size of (1.83 m × 1.83 m) is illustrated in Figure 2. For each numerical simulation, the mesh size was adopted as 10 m ×10 m × 12 m. With increasing mesh size, a little difference (< 0.5%) in computed results was found. Hence, it is justified that the adopted size is sufficient enough to overcome boundary effects. The type of element for modelling soil and pile was solid element. For allowing free movement of soil in vertical direction, roller supports were applied on vertical faces of the mesh. While restraining vertical movement of the base of the mesh, pin supports were applied. The water table level was

taken as 5 m below the ground surface same as in field conditions. Hydrostatic pore water distribution was imposed on the nodes of the mesh. For dissipation of excess pore water pressure, top surface of the mesh was imposed as free drainage boundary condition. The interaction between footings and underneath ground was assumed as frictional which is modelled by the Coulomb friction law. There are two parameters required for this model (1) frictional coefficient (μ) (2) limiting relative movement between two surfaces (γ_{lim}). The values of the μ and (γ_{lim}) were assumed as 0.35 and 5 mm, respectively (Lee et al. 2004 and Lam et al. 2009).

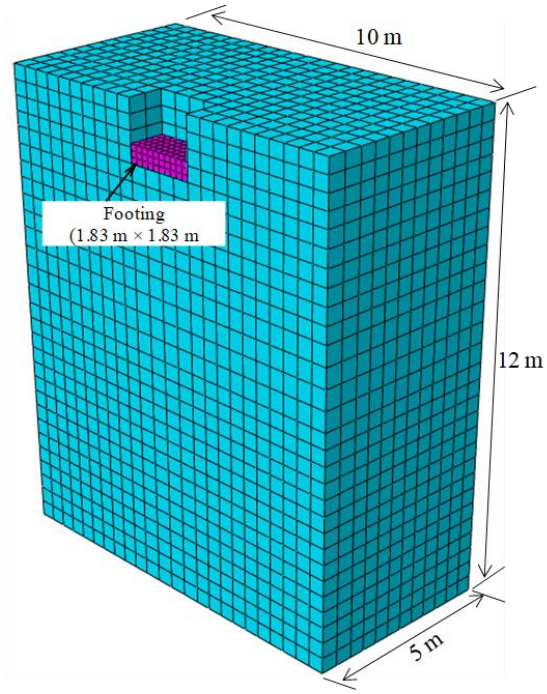

Figure 2. Three-dimensional finite element mesh

2.2. Constitutive model and its parameters

A linear elastic perfectly plastic model with Mohr-Coulomb failure criterion was used to capture soil behaviour. An associated flow rule was formulated in the soil model. The effective cohesion (c'), effective angle of friction (φ') and angle of dilation (ψ) for saturated stiff clay are taken as 5 kPa, 200 and 110, respectively. The stiffness parameters for the existing and improved ground are shown in Table 1.

Table 1. Improved parameters

Parameters	Replacement		
	20%	30%	40%
Young's Modulus (kN/m²)	10×10^3	15×10^3	20×10^3
Poisson's ratio	0.33	0.33	0.33
Dry unit weight (kN/m³)	17.0	17.5	18.0
Saturated unit weight (kN/m³)	19.0	19.5	20.0
Cohesion (c')	1.0	1.0	1.0
Friction angle (φ')	32	35	38
Permeability (m/day)	0.2	0.5	1.0

The concrete footings are assumed linear elastic with Young's modulus of 35 GPa and Poisson's ratio of 0.25. Mayne and Kulhawy's equation (given below) was used to calculate lateral earth pressure coefficient at rest K_o. The coefficient of lateral earth pressure at rest, is estimated by K0=1-sin'OCRsin'

2.3. Numerical modelling procedure

The numerical modelling procedure is summarized as follows:

1. Generate the geostatic stresses at K_0 value in the mesh for each case
2. Activate the elements of the footing
3. The footing was loaded incrementally with each increment of 1340 kN up to maximum 75 kN over a period of 24 hours.

3. Intpretation of computed results

3.1. Ultimate bearing capacity of the footings on existing silty clay

Figure 3 shows the relationship between load and settlement for each of the three different sizes of footings (i.e. 1.22 ×1.22 m², 1.83×1.83 m² and 1.22×1.83 m²). These curves were obtained from the numerical load tests performed for each footing. The estimated "yield" point (which is defined as the load-settlement curve starts to deviate from the tangent line) is also indicated in the figure. Moreover, ultimate load for each footing calculated from the bearing capacity equation given by Meyerhof [20] is also indicated in the figure for comparison.

It can be seen from the figure that the load settlement curves for each footing exhibit linear behaviour in the beginning. However, with further increment of load, non-linear characteristics of the curves were observed with a distinctive "yield" point. As the footing size increases, the yield point becomes higher. The yield point for the (1.22×1.22 m²), (1.83×1.83 m²) and (1.22×1.83 m²) footings are found to be 0.37 MN, 0.66 MN and 0.52 MN, respectively. The response of bigger of size footing was stiffer than that of smaller size footing. To be more specific, for given load the larger size footing settles less than the smaller size footing. Using tangent intersection method, the computed ultimate load for the footing of sizes (1.22×1.22 m²), (1.83×1.83 m²) and (1.22×1.83 m²) were found to be 0.59 MN, 0.90 MN and 0.98 MN, respectively. Compared to calculated bearing capacity of the three footing, it is observed that computed bearing capacity is smaller than that of calculated. This is because in analytical solution given by Meyerhof [20] assumed that soil behave as perfectly plastic. In contrast, the soil behaviour modeled in this numerical analysis is assumed as elasto-plastic material with hardening. The soil will deform due to loading as well as yield progressively because of finite element formulation. The ultimate load calculated from Meyerhof's equations for each of the three footings of sizes (1.22×1.22 m²), (1.83×1.83 m²) and (1.22×1.83 m²) were 0.66 MN, 1.4 MN and 0.92 MN, respectively. Using load settlement curves, the settlement of footings of sizes (1.22×1.22 m²), (1.83×1.83 m²) and (1.22×1.83 m²) due to their corresponding calculated ultimate loads were determined as 72 mm, 132 mm and 81 mm, respectively.

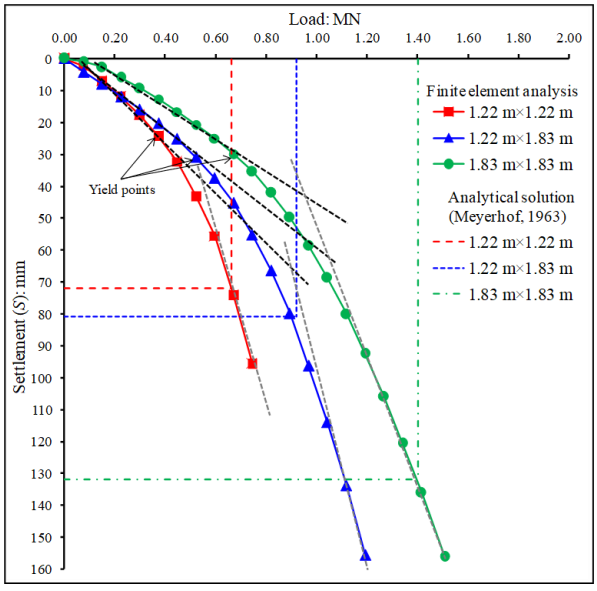

Figure 3. Load settlement curve obtained from numerical load test

3.2. Computed ground deformation mechanism and deviatoric strain

The objective of this study is to improve the bearing capacity of footing resting on existing silty ground by replacing the blended existing silty soil with granular material. Therefore, it was necessary to determine the depth of the silty ground for the replacement. To investigate the influence zone in the ground due to loading on the footing, incremental displacements vectors and plastic shear strain contours at settlement of 5% of the footing width were drawn from the computed results. Figure 4 shows the incremental displacements vectors and plastic shear strain contours for the footing size of (1.22×1.22) m² at 5% settlement. It can be seen from the figure that largest settlement of the soil occurs right underneath of the footing.

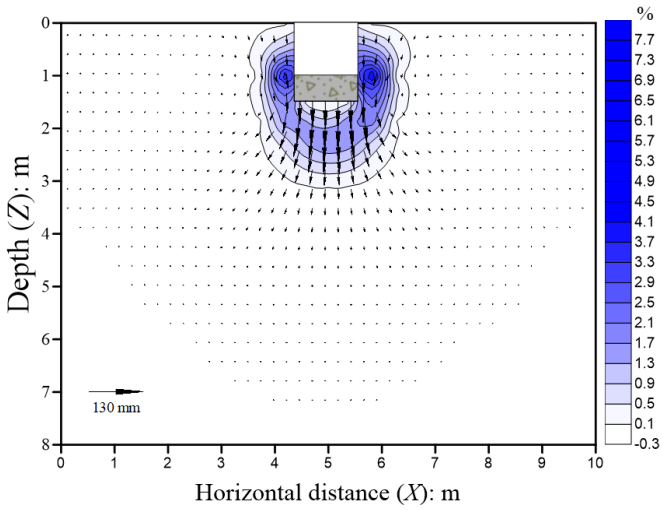

Figure 4. Computed incremental ground movement and plastic shear strain due to loading on (1.22×1.22) m² footing

Figure 5 illustratea the displacements vectors and plastic shear strain contours for the footing size of (1.83×1.83) m² at 5% settlement. It can be seen from the figure that largest settlement of the soil occurs right underneath of the footing. In addition, plastic shear strain contours are also superimposed in the figure. Significant shear strain with maximum magnitude of 7.7% has developed in log-spiral shape around the footing. From the displacement vectors and plastic shear strain contour pattern, three zones under the footing given by Terzaghi can indentified. The three zones are a triangular zone directly underneath the footing, a radial zone and a Rankine passive zone. This similarity validates the finite element results in this study. As compared to displacement and plastic shear strain influence zone for footing of size (1.22×1.22) m², the influence of loading on (1.83×1.83) m² footing becomes larger. Based on the displacement vector and shear strain contours, the influence zone in the ground due to load on the footing at 5% settlement can be identified as 4 m under the footing.

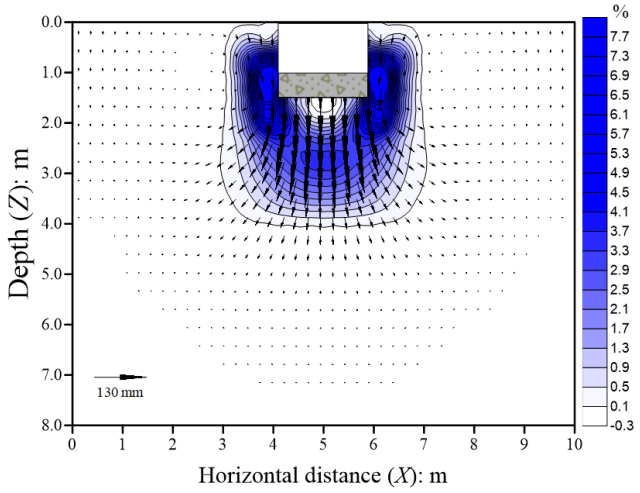

Figure 5. Computed incremental ground movement and plastic shear strain due to loading on (1.83×1.83) m² footing

Figure 6 illustrates the displacements vectors and plastic shear strain contours for the footing size of (1.22×1.83) m² at 5% settlement. It can be seen from the figure that largest settlement of the soil occurs right underneath of the footing. In addition, plastic shear strain contours are also superimposed in the figure. Significant shear strain with maximum magnitude of 7.7% has developed in log-spiral shape around the footing. From the displacement vectors and plastic shear strain contour pattern, three zones under the footing given by Terzaghi can identified. The three zones are a triangular zone directly underneath the footing, a radial zone and a Rankine passive zone. This similarity validates the finite element results in this study. As compared to displacement and plastic shear strain influence zone for footing of size (1.22×1.22) m², the influence of loading on (1.83×1.83) m² footing becomes larger. Based on the displacement vector and shear strain contours, the influence zone in the ground due to load on the footing at 5% settlement can be identified as 4 m under the footing.

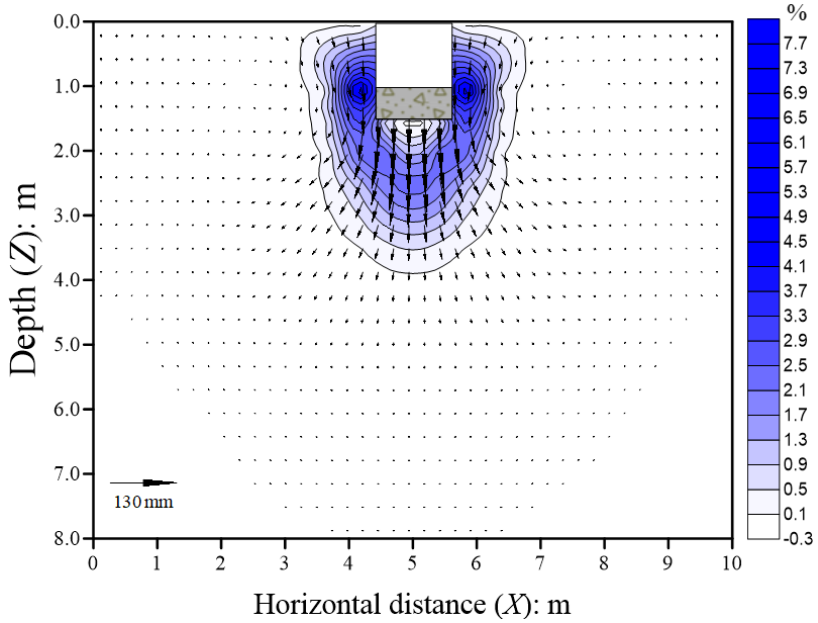

Figure 6. Computed incremental ground movement and plastic shear strain due to loading on (1.22×1.83) m² footing

3.3. Imroved ultimate bearing capacity

The bearing capacity of the footings was improved by blended existing silty ground up to 4 m (determined from plastic strain contours) by granular material. The percentage of blended granular material was 20%, 30% and 40% of silty soil. After blending, the mix was compacted at targeted degree of compaction. Subsequently, numerical load tests were conducted to compare the ultimate bearing capacity after improved ground.

3.3.1. Improved ultimate bearing capacity of footing size (1.22×1.22) m²

Figure 7 shows the load versus settlement curves for the footing of size (1.22×1.22) m² resting on the improved ground (i.e. with 20%, 30% and 40% replacement). For comparison, the load settlement curve obtained from the load test of the footing founded on existing silty ground is also included in the figure.

Owing to increased stiffness of existing silty clay blended with granular material, the response of load settlement curve was found to be quite stiff. To be specific, at a given load the settlement of footing on the improved ground was smaller than that on silty ground. The smallest settlement of the footing was calculated when footing was founded on the ground with 40% replacement. At given settlement of 72 mm, the percentage improvement in ultimate bearing capacity was computed as 45%, 68% and 91% for the footing of the size (1.22×1.22) m² founded 20%, 30% and 40% blended silty clay with granular material, receptively. With factor of safety of 1.5, the working loads were determined as 0.64 MN, 0.74 MN and 0.84 MN.

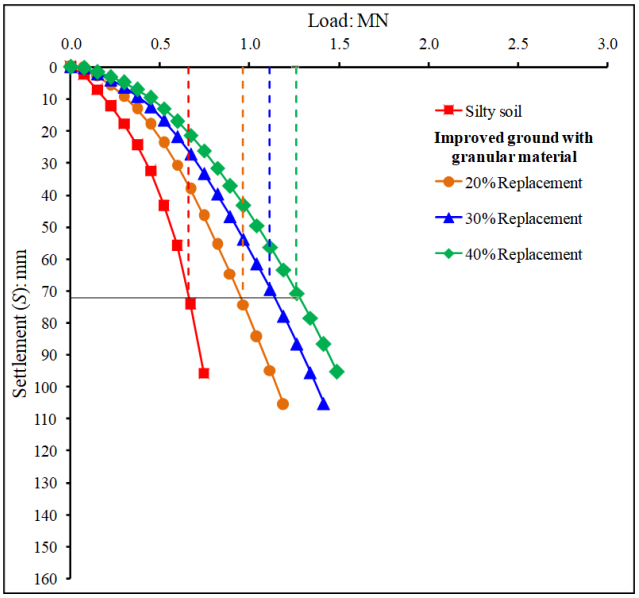

Figure 7. Load settlement for the footing of size (1.22×1.22) m² founded on improved ground

3.3.2. Improved ultimate bearing capacity of footing size (1.83×1.83) m²

Figure 8 shows the load versus settlement curves for the footing of size (1.83×1.83) m² resting on the improved ground (i.e. with 20%, 30% and 40% replacement). For comparison, the load settlement curve obtained from the load test of the footing founded on existing silty ground is also included in the figure. Owing to increased stiffness of existing silty clay blended with granular material, the response of load settlement curve was found to be quite stiff. To be specific, at a given load the settlement of footing on the improved ground was smaller than that on silty ground. The smallest settlement of the footing was calculated when footing was founded on the ground with 40% replacement. At given settlement of 132 mm (discussed in section 4.3), the percentage improvement in ultimate bearing capacity was computed as 54%, 78% and 89% for the footing of the size (1.83×1.83) m² founded 20%, 30% and 40% blended silty clay with granular material, receptively. With factor of safety of 1.5, the working loads were determined as 1.44 MN, 1.66 MN and 1.77 MN.

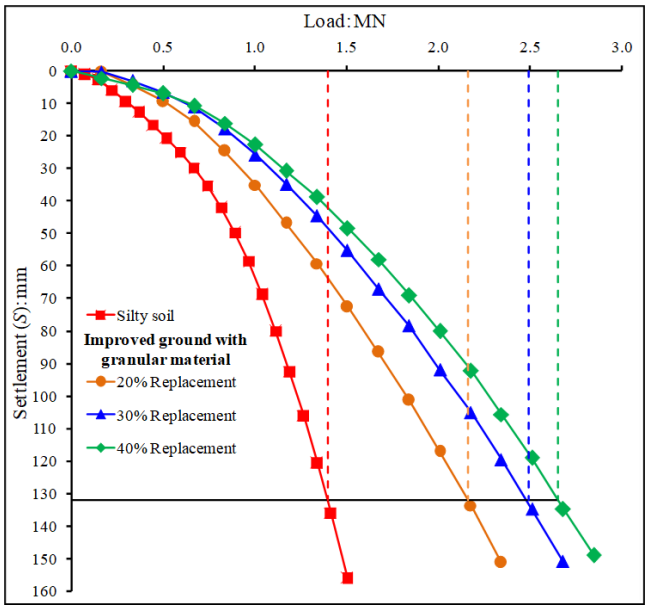

Figure 8. Load settlement for the footing of size (1.83×1.83) m² founded on improved ground

3.3.3. Improved ultimate bearing capacity of footing size (1.22×1.83) m²

Figure 9 shows the load versus settlement curves for the footing of size (1.22×1.83) m² resting on the improved ground (i.e. with 20%, 30% and 40% replacement). For comparison, the load settlement curve obtained from the load test of the footing founded on existing silty ground is also included in the figure. Owing to increased stiffness of existing silty clay blended with granular material, the response of load settlement curve was found to be quite stiff. To be specific, at a given load the settlement of footing on the improved ground was smaller than that on silty ground. The smallest settlement of the footing was calculated when footing was founded on the ground with 40% replacement. At given settlement of 81 mm (discussed in section 4.3), the percentage improvement in ultimate bearing capacity was computed as 42%, 68% and 83% for the footing of the size (1.22×1.83) m² founded 20%, 30% and 40% blended silty clay with granular material, receptively. With factor of safety of 1.5, the working loads were determined as 1.12 MN, 1.00 MN and 1.83 MN.

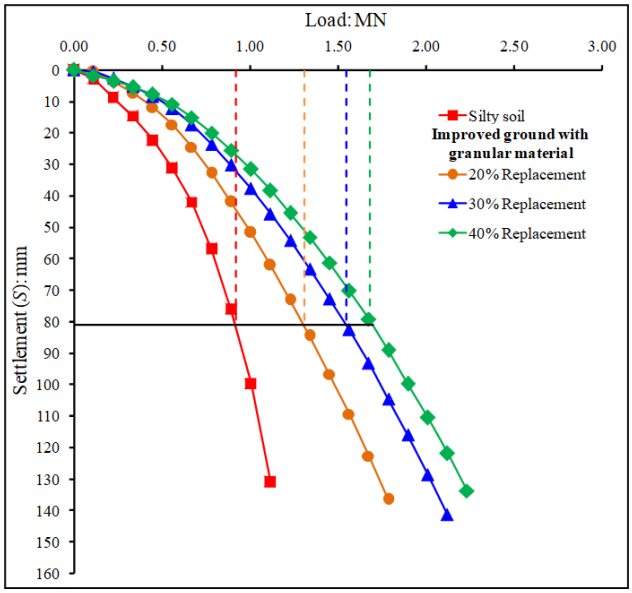

Figure 8. Load settlement for the footing of size (1.22×1.83) m² founded on improved ground

4. Conclusions

To assess the bearing capacity of shallow foundations, three-dimensional finite element analysis was conducted on footings of three sizes (1.83 m × 1.83 m, 1.22 m × 1.22 m, and 1.22 m × 1.83 m) placed on both existing and improved ground. The analysis compared the performance of the footings on the original soil with those placed on the enhanced ground. A linear elastic perfectly plastic model incorporating the Mohr-Coulomb failure criterion was used to accurately simulate soil behavior during the study. Based on the ground conditions and geometries, the following conclusions can be drawn.

1. As the footing size increases, the yield point becomes higher. The yield point for the (1.22×1.22 m²), (1.83×1.83 m²) and (1.22×1.83 m²) footings are found to be 0.37 MN, 0.66 MN and 0.52 MN, respectively.
2. Using tangent intersection method, the computed ultimate load for the footing of sizes (1.22×1.22 m²), (1.83×1.83 m²) and (1.22×1.83 m²) were found to be 0.59 MN, 0.90 MN and 0.98 MN, respectively.
3. Using load settlement curves, the settlement of footings of sizes (1.22×1.22 m²), (1.83×1.83 m²) and (1.22×1.83 m²) due to their corresponding calculated ultimate loads were determined as 72 mm, 132 mm and 81 mm, respectively.
4. Based on the displacement vector and shear strain contours, the influence zone in the ground due to load on all the three footings at 5% settlement can be identified as 4 m under the footing.
5. The percentage improvement in ultimate bearing capacity was computed as 45%, 68% and 91% for the footing of the size (1.22×1.22) m² founded 20%, 30% and 40% blended silty clay with granular material, receptively. With factor of safety of 1.5, the working loads were determined as 0.64 MN, 0.74 MN and 0.84 MN. With factor of safety of 1.5, the working loads were determined as 0.64 MN, 0.74 MN and 0.84 MN.

6. The percentage improvement in ultimate bearing capacity was computed as 54%, 78% and 89% for the footing of the size (1.83×1.83) m² founded 20%, 30% and 40% blended silty clay with granular material, receptively. With factor of safety of 1.5, the working loads were determined as 1.44 MN, 1.66 MN and 1.77 MN.
7. The percentage improvement in ultimate bearing capacity was computed as 42%, 68% and 83% for the footing of the size (1.22×1.83) m² founded 20%, 30% and 40% blended silty clay with granular material, receptively. With factor of safety of 1.5, the working loads were determined as 1.12 MN, 1.00 MN and 1.83 MN.

References

1. Salencon J. (2003), "Bearing capacity of strip footings with horizontal confinement", C. R. Me´ c. Vol. 331, No.5, pp.319–324.
2. Villalobos F, Byrne B.W, Houlsby G.T, Martin C.M. (2003), "Bearing capacity tests of scale suction caisson footings on sand, experimental data", data report FOT005/1, Civil Engineering Research Group, Department of Engineering Science, The University of Oxford,
3. Mahiyar H, Patel A.N. (1997), "The effect of lateral confinement on the bearing capacity of fine sand", Indian Geotech. J. New Delhi, Vol. 22, No.4, pp.226–234.
4. Singh V. K et al. (2007), "Effect of soil confinement on ultimate bearing capacity of square footing under eccentric inclined load", Electron. J. Geotech. Eng. 12 1–14 (Bundle. E).
5. El Sawwaf M.E.I, Nazer A. (2005), Behavior of circular footings on confined granular soil, J. Geotech. Geoenviron. Eng. ASCE, Vol.131, No. 3, pp.359–366.
6. Ortiz J.M.R. (2001), "Strengthening of foundations through peripheral confinement, in: Proceedings of 15th the International Conference on Soil Mechanics and Geotechnical Engineering, Netherlands, Vol. 1, pp. 779–882.
7. Al-Aghbari M.Y, Mohamedzein Y.E.-A. (2004), "Bearing capacity of strip foundations with structural skirts", J. Geotech. Geol. Eng. Vol. 22, No. 1, pp 43–57.
8. Rajagopal K, Krishnaswamy N, Latha G. (1999), "Behavior of sand confined with single and multiple geocells", Geotext. Geomembr., Vol. 17, pp.171–184.
9. Dash S.K, Krishnaswamy N, Rajagopal K, (2001), "Bearing capacity of strip footing supported on geocell-reinforced sand", Geotext. Geomembr. Vol.19, pp.235–256.
10. Dash S.K, Sireesh S, Sitharam T.G, (2003), "Behavior of geocell reinforced sand beds under circular footing", Ground Improv. Vol. 7, pp. 111–115.
11. Mukhtiar Ali Soomro, Shaokai Xiong, Naeem Mangi, Dildar Ali Mangnejo, Sharafat Ali Darban (2024), "Enhancing foundation bearing capacity in waterlogged ground for sustainable building construction", Geomechanics and Engineering, Vol. 39, No. 4, pp. 407-423.
12. Chauhan M.S, Mittal S, Mohanty B, (2008) "Performance evaluation of silty sand sub-grade reinforced with fly ash and fiber" India.
13. Hyunwook, K. and William, G. (2009) "Finite element cohesive fracture modeling of airport pavements at low temperatures", Elsevier Scientific Publishing, Cold Regions Science and Technology, Vol. 57, pp. 123-130.
14. Hamza Gullu (2012)" A numerical study on geotextile stabilized highway embankment under vibration loading".
15. Mostafa Deep Hashem (2013) "Numerical Modeling of Flexible Pavement Constructed on Expansive Soils". European International Journal of Science and Technology, Vol. 2, No. 10, pp. 19-34
16. Ayman A. Abed, (2008), "Numerical Modeling of Expansive Soil Behavior", Ph.D. thesis, Institute for geotechnical, Stuttgart University, Germany.
17. Djellali A., Ounis A. and Saghafiq., (2012), "Behavior of Flexible Pavements on Expansive Soils", Journal of Transportation Engineering, Vo1.1, No.1, pp. 1-14.
18. Bolton, M.D. (1986). The strength and dilatancy of sands. Geotechnique, 36 (1), 65-78.
19. Ottosen, N.S. & Petersson, H. (1992). Introduction to the finite element method. New York: Prentice Hall.
20. Meyerhof, G. G. (1963). "Some recent research on the bearing capacity of foundations", Canadian Geotechnical Journal, Vol. 1, No. 1, pp. 16–26.